AGU100 ADVANCING EARTH AND SPACE SCIENCE

Water Resources Research

RESEARCH ARTICLE

10.1029/2018WR023352

Key Points:
- The study results show that water repellency reduces water vapor sorption by kaolinite and montmorillonite minerals
- Trace levels of hydrophobicity-inducing organic agents affected vapor sorption even when liquid water contact angles were unaffected
- Decreased surface area (from aggregation) and altered surface potential were the primary causes of reduced water vapor sorption

Supporting Information:
- Supporting Information S1

Correspondence to:
R. D. Stewart,
ryan.stewart@vt.edu

Citation:
Chen, J., Shang, C., Eick, M. J., & Stewart, R. D. (2018). Water repellency decreases vapor sorption of clay minerals. *Water Resources Research*, *54*. https://doi.org/10.1029/2018WR023352

Received 22 MAY 2018
Accepted 9 AUG 2018
Accepted article online 21 AUG 2018

Water Repellency Decreases Vapor Sorption of Clay Minerals

Jingjing Chen[1], Chao Shang[1], Matthew J. Eick[1], and Ryan D. Stewart[1]

[1]Department of Crop and Soil Environmental Science, Virginia Tech, Blacksburg, VA, USA

Abstract As soils become dry, water primarily exists as vapor that adsorbs to and desorbs from particle surfaces. The drying process also often enhances soil water repellency, yet the effects of repellency on soil water vapor sorption and exchange are not well understood. The objective of this study was to quantify the water vapor sorption dynamics of two minerals (Ca^{2+} saturated kaolinite and montmorillonite), in which water repellency was induced using two organic agents: cetyl trimethylammonium bromide (~4% by mass) and stearic acid (0.5%, 5%, 10%, 20%, and 35% by mass). Samples were then analyzed for water vapor sorption isotherms, solid-water contact angles, organic carbon content, mineral surface morphology, hydrophobic functional groups (using Fourier transform infrared spectroscopy), zeta potential, and particle size distributions. The results showed that the water repellent treatments altered particle surface potentials and decreased surface areas relative to the controls. As a result, those samples adsorbed significantly less water and had less hysteresis between adsorption and desorption isotherms than the nontreated controls ($p < 0.05$). Differences in water adsorption were most pronounced for water activities >0.6, where hydrophobic compounds may have inhibited water vapor condensation, even at low concentrations. In contrast, solid-water contact angles were small in montmorillonite treatments with <10% stearic acid, suggesting that low levels of hydrophobic compounds may have greater effect on vapor sorption compared to liquid water imbibition. Altogether, these results imply that repellency may reduce water retention in dry soils and enhance water vapor losses.

Plain Language Summary Many soils become water repellent as they dry, such that water drops cannot penetrate the soil surface, yet specific interactions between water vapor and water-repellent soil particles remain poorly understood. In this study we applied two different chemicals to clay minerals to induce varying degrees of water repellency and then measured the ability of treated particles to adsorb and rerelease water vapor. The water repellent minerals adsorbed less water vapor than nontreated minerals, because the applied chemicals (1) reduced the ability of water vapor to access wettable sites on mineral surfaces, (2) caused particles to aggregate together, further limiting the surface area available to water vapor, and (3) altered the ability of minerals to attract water vapor onto their exposed surfaces. These findings suggest that soil water repellency may enhance water vapor losses from drying soils, yet more study is needed to verify that these results translate to natural field soils.

1. Introduction

Soil water repellency can decrease soil infiltration capacity (Steenhuis et al., 2005) and water holding capacity (Orfanus et al., 2014), enhance overland flow and flooding (Larsen et al., 2009; Miyata et al., 2007), accelerate development of preferential flow (Ritsema et al., 1993), and in some cases increase agrichemical leaching (Letey, 2001). These alterations may drive soil erosional processes and increase the mobility of surface-bound pollutants, with the potential to reduce water quality and degrade aquatic ecosystems (Doerr et al., 2000; Kidron, 2015). Soil water repellency has become more prevalent in recent years due to drought conditions and wildfires (Abatzoglou & Williams, 2016; Dai, 2011; Dennison et al., 2014; Granged et al., 2011), as well as changes in agriculture management practices, such as long-term applications of feedlot manure (Miller et al., 2017; Valolahti et al., 2015). Global climate change effects such as rising temperatures and shifting precipitation patterns may also result in more widespread development of repellency (Goebel et al., 2011). Thus, it is critical to understand how soil water repellency influences hydrological processes.

Previous research has focused on interactions between soils and liquid water, for example, by quantifying how water repellency can increase solid-water contact angles and thereby reduce soil capillarity (Leelamanie et al., 2008) and water infiltration (Granged et al., 2011). In contrast, it is not yet well understood if and how changes in particle surface properties induced by water repellency affect soil water vapor sorption

and exchange. Water vapor sorption/desorption dynamics—where vapor molecules bind to/release from mineral surfaces—form a primary control on near-surface moisture distributions in soils as they dry (Schneider & Goss, 2012). The drying process can also enhance repellency (Doerr & Thomas, 2000), meaning that the potential exists for feedbacks between soil water repellency formation and vapor exchange. Such mechanisms may be particularly relevant in arid and semiarid regions, where water primarily exists in the vapor phase (Tuller & Or, 2005).

Water vapor sorption onto particle surface is regulated by adhesion forces (i.e., van der Waals attraction, electrostatic, and acid-base interactions; Derjaguin et al., 1987), which are controlled by particle surface characteristics such as surface area (Arthur et al., 2015; Tuller & Or, 2005), surface charge (Arthur et al., 2016; Leão & Tuller, 2014; Woodruff & Revil, 2011), and surface-free energy (Leão & Tuller, 2014; Parks, 1984). Each of these properties may be altered by the introduction of hydrophobic surface functional groups. Water vapor sorption on mineral surfaces generally occurs in three stages: (1) water vapor monolayer adsorption/desorption on external surfaces; (2) water vapor interlayer and multiple layer adsorption/desorption; and (3) capillary condensation, which refers to the growth and coalescence of water into liquid-like overlayers (Yeşilbaş & Boily, 2016). The monolayer regime occurs when water activity (a_w) ranges from near 0 to between 0.19 and 0.53, depending on clay mineral type and properties (Newman, 1983; Puri & Murari, 1964; Quirk & Murray, 1999). In both kaolinite and montmorillonite, a monolayer forms on external surfaces until a_w reaches ~0.2 (Hatch et al., 2012). Swelling 2:1 minerals (e.g., montmorillonite) also have internal monolayer adsorption, which occurs in the range of water activities $0.2 < a_w < 0.6$ (Arthur et al., 2018; Quirk & Murray, 1999). Several studies have demonstrated that water molecules do not form uniform monolayers on particle surfaces, as polar molecules tend to cluster around cation sites (Lu & Khorshidi, 2015; Quirk, 1955). This effect is particularly notable in minerals with high surface area (e.g., smectite), where the monolayer formation partially overlaps with cation hydration. Water vapor multilayer/interlayer adsorption also develops when a_w ranges from 0.2 to 0.6; this process is dominated by both mineral structural properties and water-water and water-cation interactions on mineral surfaces (Branson & Newman, 1983; Ormerod & Newman, 1983). Water films begin to demonstrate liquid-like behavior when $a_w > 0.55$ (Arthur et al., 2016), while capillary condensation is the primary form of soil hydration for $a_w > 0.6$ (Hatch et al., 2012).

Because it includes information about all three hydration stages, the soil water vapor sorption isotherm is a useful tool for characterizing water vapor dynamics in soil. Isotherm curves express soil water vapor sorption in terms of soil water content (i.e., mass of water adsorbed per mass of soil) as a function of a_w at a constant temperature. In general, water vapor sorption isotherms follow unique paths in response to variations in soil water energy levels and form hysteresis loops that are contained between two master adsorption and desorption curves. Hysteresis in a water vapor sorption isotherm indicates that vapor adsorption onto the particle surface requires less energy than vapor release (Laird et al., 1995). This result may be attributed to both particle surface and cation hydration, which are dominated by particle surface charge, energy, and area (Lu & Khorshidi, 2015). Hysteresis in dry-end water retention ($a_w < 0.95$) therefore can characterize the interactions between water vapor and solid surfaces (Prunty & Bell, 2007).

In the past, it has been assumed that water vapor moves freely in soil regardless of any water repellency that the soil may exhibit (Imeson et al., 1992; Miyamoto et al., 1972). More recent research has indicated that hydrophobic substances in soil may reduce the water vapor movement at very low water activities (Arthur et al., 2014; Dagnelie et al., 2010; Inagaki et al., 1996; Maaz et al., 2016), but the underlying interactions and mechanisms have not yet been critically examined. The overall objective of this study was to quantify the effects of particle surface hydrophobicity on water vapor sorption characteristics. By comparing water vapor sorption characteristics with variations in particle surface properties, we intend to improve the general understanding of the effects of soil water repellency on water vapor sorption and exchange.

2. Materials and Methods

2.1. Sample Preparation and Treatments

We conducted a set of experiments using model soil systems by measuring soil water vapor sorption isotherms for two mineral types—kaolinite (Georgian kaolinite, KGA) and montmorillonite (Wyoming Na-rich montmorillonite, SWY)—that had been mixed with varying types and amounts of organic compounds to

Table 1
Average of pH and Total Organic Carbon (TOC) of Ca^{2+}-Kaolinite (KGA) and Ca^{2+}-Montmorillonite (SWY) Minerals Treated with Different Mass Percentages of Stearic Acid (SA) and Saturated by Cetyl Trimethylammonium Bromide (CTAB)

	pH		TOC g 100 g^{-1}	
Treatments	KGA	SWY	KGA	SWY
Control	5.4 ± 0.01	6.9 ± 0.1	0.1 ± 0.01	0.1 ± 0.02
0.5% SA	5.3 ± 0.2	6.6 ± 0.1	0.5 ± 0.03	0.4 ± 0.1
5% SA	5.3 ± 0.5	5.9 ± 0.04	4.2 ± 0.03	3.5 ± 0.8
10% SA	5.3 ± 0.5	6.3 ± 0.7	6.2 ± 0.6	6.9 ± 0.3
20% SA	5.0 ± 0.5	6.0 ± 0.6	13.5 ± 0.5	13.7 ± 0.3
35% SA	4.8 ± 0.3	5.9 ± 0.01	23.8 ± 0.9	24.4 ± 0.3
CTAB	5.2 ± 0.2	5.8 ± 0.3	1.2 ± 0.2	3.4 ± 0.6

Note. ± values represent standard errors (n = 3).

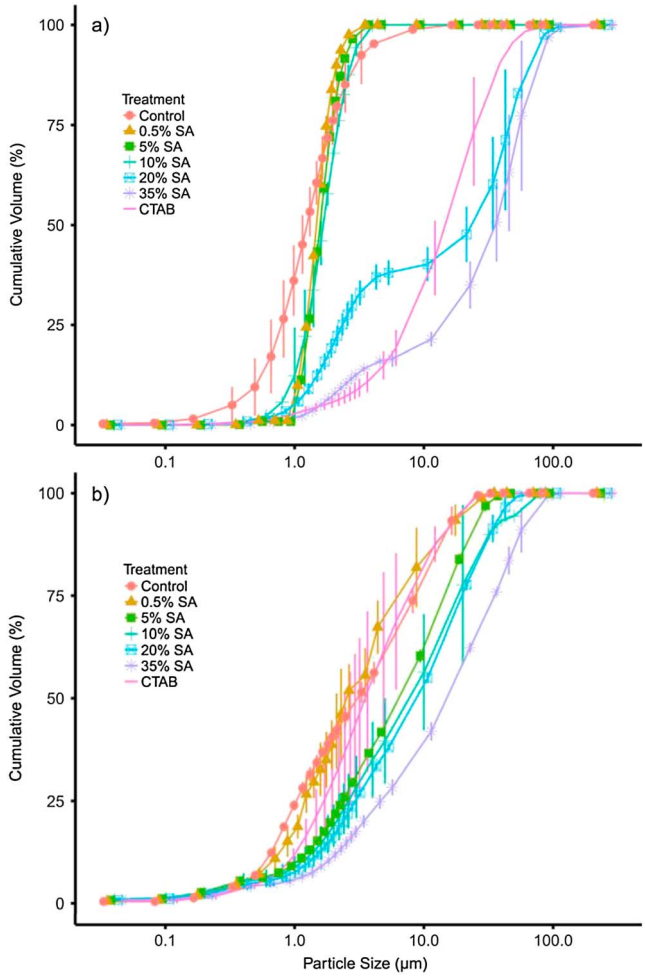

Figure 1. Particle size distributions of (a) Ca^{2+}-montmorillonite and (b) Ca^{2+}-kaolinite minerals treated by 0% (control), 0.5%, 5%, 10%, 20%, and 35% stearic acid (SA) and saturated by cetyl trimethylammonium bromide (CTAB). Error bars represent standard errors (n = 3).

induce hydrophobicity. The minerals came from the Clay Mineral Society Source Clays Repository and were prepared by sequentially washing the samples with sodium acetate (NaOAc), hydrogen peroxide (H_2O_2), and sodium dithionite ($Na_2S_2O_4$) to remove soluble salts, carbonate, organic matter, and free iron oxides. The clay fraction (<2 μm) was obtained by centrifuging the water suspension of each mineral at 60 g for 6 min. The purified clays were then washed with a calcium chloride (Ca_2Cl) solution and rinsed with deionized water to prepare Ca^{2+}-saturated samples.

To establish water repellency in the model systems, the monoionic clay samples were mixed with one of two hydrophobicity-inducing agents: stearic acid (SA) or cetyl trimethylammonium bromide (CTAB). SA is a fatty acid commonly found in soils consisting of an 18-carbon chain with a carboxylic acid group [$CH_3(CH_2)_{16}COOH$]. CTAB is a cation surfactant commonly used in industrial processes that contains a 16-carbon chain and a quaternary ammonium functional groups on the other end ([$(C_{16}H_{33})$ N $(CH_3)_3]^+Br^-$). The following hydrophobic treatments were used, with the relative mass of adsorbed compound indicated: 0% (control), 0.5% SA, 5% SA, 10% SA, 20% SA, 35% SA, and CTAB (saturated). Diethyl ether was used to dissolve the SA before application to the minerals (Leelamanie & Karube, 2007; Lichner et al., 2006), while distilled water was used as a medium to apply CTAB following the procedure of Zhu et al. (1998). Three replicates were used for each combination of mineral type and hydrophobic treatment (n = 3).

2.2. Sample Characterization and Analysis

All treated samples were divided into subsamples to analyze physicochemical properties. Particle zeta potential was measured using a Zetasizer 3000HS (Malvern Instruments, Worcestershire, UK) with the following parameters: temperature = 25 °C, dielectric constant = 79.0, and viscosity = 0.890. Particle size distribution was measured using a CILAS 1190 particle size analyzer (CILAS, Inc., Orleans, France), following the sample preparation procedure of Gee and Bauder (1986). Total organic carbon of samples was detected by a C/N analyzer (VarioMax CNS macroelement analyzer, Elementar Analytical Systems GmbH, Hanau, Germany). The occurrence of functional groups of SA and CTAB contributing to hydrophobicity was examined by a Nicolet 8700 Fourier transform infrared (FTIR) spectrometer (ThermoFisher Scientific, Inc., Waltham, USA), following the sample preparation procedure of Schwen et al. (2015). An environmental scanning electron microscope (FEI Quanta 600 FEG, Hillsboro, USA) was used to examine the morphology and organization of the particles under the different hydrophobic treatments. Sample pH was measured in 1:5 soil to water suspensions using a 3100 M pH meter (OHAUS, Inc., Parsippany, USA).

Solid-water contact angles were measured for all samples following the method of Whelan et al. (2015) and Bachmann et al. (2000). Briefly, a layer of mineral grains was fixed on a glass microscope slide with double-sided adhesive tape by sprinkling, gentle pressing, and removing loose material. Deionized water droplets with a volume of 20 μL were placed on the sample and photographed within 3 s under a constant temperature (25 °C). The contact angle was calculated using ImageJ software (version 1.50i). Note that a contact angle of ~0° indicates a hydrophilic surface, a contact angle between ~0 and 90° indicates subcritical water repellency, and a contact angle larger than 90° indicates critical water repellency, also known as hydrophobicity (Bachmann et al., 2000).

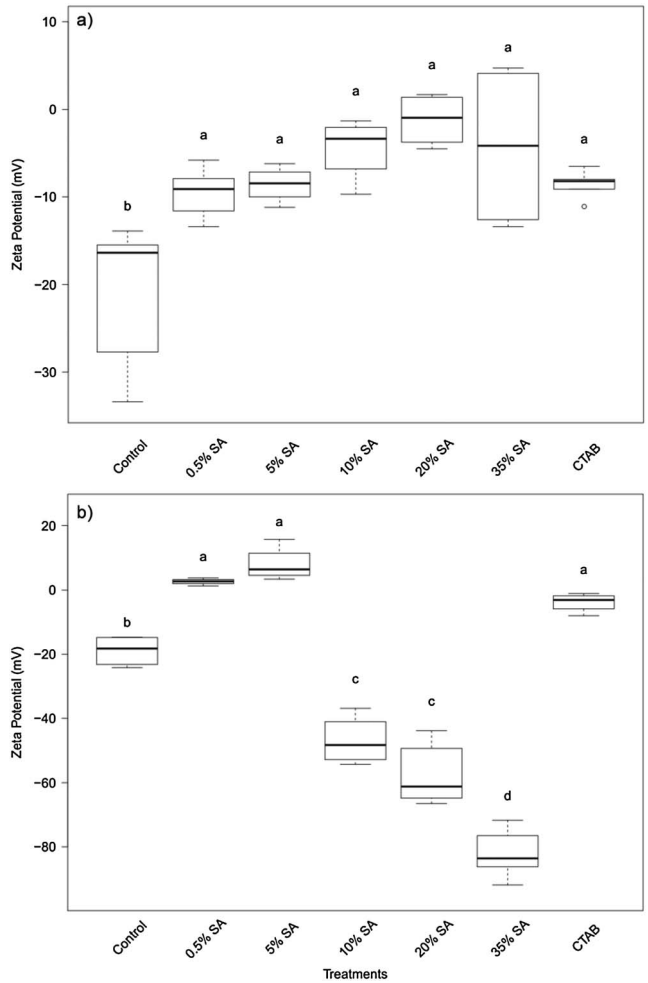

Figure 2. Zeta potential of (a) Ca^{2+}-montmorillonite and (b) Ca^{2+}-kaolinite treated by 0% (control), 0.5%, 5%, 10%, 20%, and 35% of stearic acid (SA) and saturated by cetyl trimethylammonium bromide (CTAB; $n = 3$). The upper whiskers refer to the values ranging from the upper quartile to the highest data point that is less than the upper quartile plus 1.5 times the interquartile (Q3 + 1.5 IQR); the lower whiskers refer to the values ranging from the lower quartile down to the lowest data point that is greater than the lower quartile minus 1.5 times the interquartile (Q1 − 1.5 IQR). Different letters denote significant differences between mean values (ANOVA with Tukey's HSD, $p < 0.05$). ANOVA = analysis of variance; HSD = honestly significant difference.

Water vapor sorption isotherms were measured using a vapor sorption analyzer (METER Group, Inc., Pullman, USA) with the following settings: adsorption followed by desorption over the water activity range of 0.05–0.95, resolution of 0.02, Dynamic Dewpoint Isotherm mode, and temperature = 25 °C. Approximately 2.0 g air-dried sample was used in each measurement. In order to provide all samples with the same initial condition and thereby avoid the effects of historical wetting and drying states on water vapor sorption isotherms, all of the prepared samples were conditioned with P_2O_5 in a glass desiccator for 3 days prior to the tests. Water content was determined at the conclusion of the isotherm measurements by oven drying the samples for 48 hr at 105 °C.

For analysis, the isotherms were divided into three regions that represent distinct modes of solid-water interaction: external monolayer sorption for $a_w \leq 0.2$, multilayer/interlayer sorption for the range $0.2 < a_w < 0.6$, and capillary condensation for $a_w \geq 0.6$. Differences in adsorbed and desorbed water were calculated for each region (e.g., adsorbed water between 0.2 and 0.6 was determined as water content at $a_w = 0.6$ minus water content at $a_w = 0.2$).

Isotherms were also analyzed for the total area associated with hysteresis:

$$\text{Hysteretic Area} = \int_{a_{w,i}}^{a_{w,f}} (\theta_{\text{des}} - \theta_{\text{ads}}) da_w \tag{1}$$

where $a_{w,i}$ and $a_{w,f}$ represent the initial and final water activities, and θ_{des} and θ_{ads} are the respective water contents of the desorbed and adsorbed water (both as functions of a_w).

2.3. Statistical Analysis

Statistical analysis was performed using R software (version 3.5.0) and Python (version 3.6). All data were tested for normality and homogeneity of variances prior to analysis using a one-way analysis of variance (ANOVA) with Tukey honestly significant difference. Differences were considered significant for α 0.05.

3. Results

3.1. Mineral pH and Organic Carbon Contents of Treated Samples

Mineral pH ranged from 5.4 to 4.8 in the KGA treatments and from 6.9 to 5.9 in the SWY treatments (Table 1). ANOVA showed that the pH did not significantly vary for either mineral because of the addition of the repellency-inducing chemicals ($p > 0.05$).

Next, we used three different methods to examine the interactions of SA and CTAB with kaolinite and montmorillonite. In the first approach, we measured the total amount of carbon associated with each treatment. These results showed that the amount of SA present for a given treatment was generally consistent between minerals (e.g., the 20% SA treatment had an actual carbon contents of 13.5% by mass for kaolinite and 13.7% for montmorillonite; Table 1). The CTAB was more variable, with 1.9% CTAB (carbon content = 1.2%) adsorbed onto the kaolinite at saturation versus 5.4% CTAB (carbon content = 3.4%) adsorbed onto the montmorillonite at saturation. The retention of CTAB on kaolinite may be attributed in part to the presence of smectite impurities.

In the second approach, we used FTIR spectroscopy to identify hydrophobic functional groups on the mineral surfaces. Note that full FTIR results and analyses are presented in the supporting information (Ellerbrock & Gerke, 2016; Lin et al., 2016; Nobrega et al., 2012; Santos et al., 2014; Simkovic et al., 2008; Youssef et al., 2013). In brief, minerals treated with CTAB showed evidence of hydrophobic aliphatic methyl and methylene

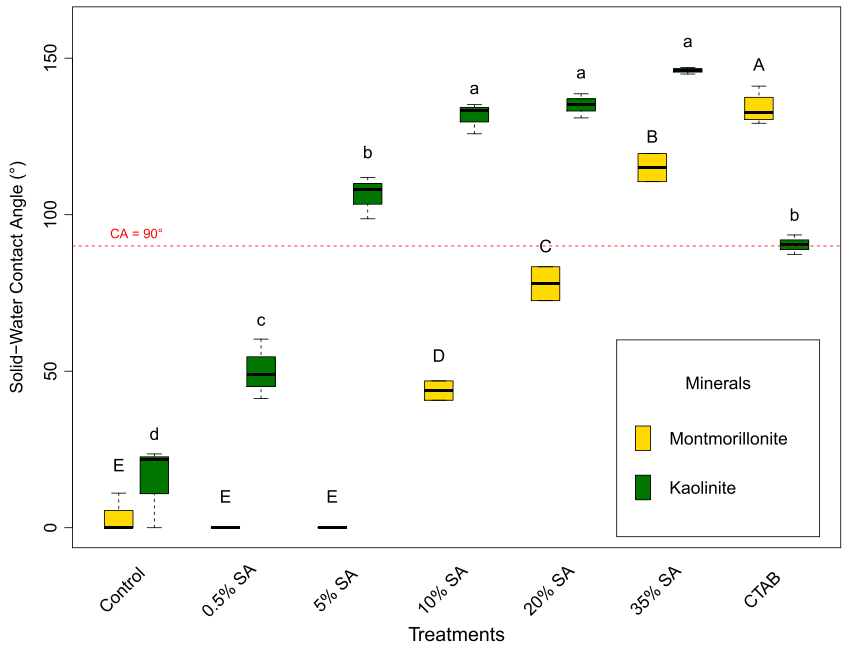

Figure 3. Solid-water contact angle measured for Ca^{2+}-montmorillonite and Ca^{2+}-kaolinite minerals treated by 0% (control), 0.5%, 5%, 10%, 20%, and 35% of stearic acid (SA) and saturated by cetyl trimethylammonium bromide (CTAB; $n = 3$). The upper whiskers refer to the values ranging from the upper quartile to the highest data point that is less than the upper quartile plus 1.5 times the interquartile (Q3 + 1.5 IQR); the lower whiskers refer to the values ranging from the lower quartile down to the lowest data point that is greater than the lower quartile minus 1.5 times the interquartile (Q1 − 1.5 IQR). Different lowercase letters denote significant differences between mean values for kaolinite samples, and different capital letters denote significant differences between mean values for montmorillonite samples (ANOVA with Tukey's HSD, $p < 0.05$). The red line indicates a contact angle (CA) of 90°, used here to differentiate between subcritically water repellent and hydrophobic conditions. ANOVA = analysis of variance; HSD = honestly significant difference.

functional groups, with the CTAB molecules becoming fixed within the montmorillonite interlayer spaces via electrostatic interaction. At low concentrations (i.e., SA ≤ 10% for kaolinite and SA ≤ 5% for montmorillonite), the SA treatments showed evidence of hydrophobic methyl and methylene groups; at higher SA concentrations hydrophilic (carboxyl) groups were also detected. This latter observation suggests the formation of free-phase SA.

In the third approach, we used an environmental scanning electron microscope to characterize SA- and CTAB-treated clays (full details and results are again presented in the supporting information). In summary, these images showed that at low concentrations, CTAB and SA formed compact and smooth coatings on the minerals (Figure S2). However, higher SA concentrations (i.e., ≥ 10% in kaolinite and ≥ 20% in montmorillonite) caused the surfaces to become rough and irregular, likely due to the formation of SA in free phase (as seen in the small white particles on the mineral surfaces in Figures S2a4 and S2a5, and S2b4 and S2b5). Kaolinite had more free-phase SA than montmorillonite due to its lower surface charge and smaller surface area.

3.2. Particle Size Distribution

Particle size distributions of all treatments are shown in Figure 1. There were no significant differences between the controls and minerals treated with low SA concentrations (i.e., SA ≤ 10% for montmorillonite, and SA ≤ 5% for kaolinite). Increased SA concentrations caused the particle size distributions to shift to the right compared to the controls, indicating that the particle sizes became larger due to particle aggregation. In addition, free-phase SA may have formed agglomerates in the treatments with high SA concentrations (as seen in Figure S2). For montmorillonite, the CTAB treatment showed a significant shift toward larger particle sizes, which may suggest aggregation as well as a possible interlayer expansion in the montmorillonite sheets due to CTAB molecules entering the clay structure. For kaolinite, the aggregation was relatively minor for CTAB treatment, which may relate to the small amount of CTAB adsorbed by kaolinite.

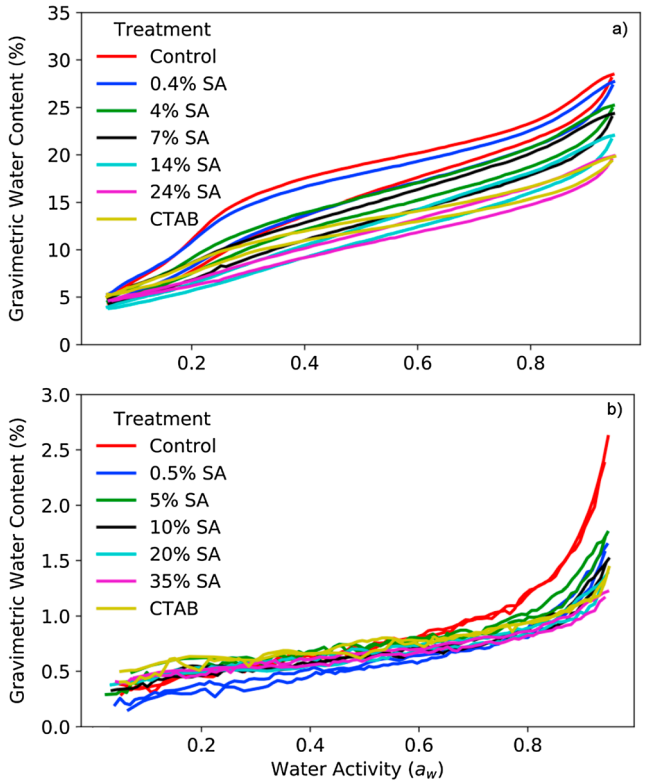

Figure 4. Mean of water vapor sorption isotherms of (a) Ca^{2+}-montmorillonite and (b) Ca^{2+}-kaolinite treated by 0% (control), 0.5%, 5%, 10%, 20%, and 35% of stearic acid (SA) and saturated by cetyl trimethylammonium bromide (CTAB; $n = 3$).

3.3. Surface Potential (Zeta Potential)

The mineral zeta potentials were altered by the treatments with SA and CTAB (Figure 2). The average zeta potential of the untreated minerals was −18.90 (kaolinite) and −20.51 mV (montmorillonite), which were similar to the values reported by Leroy et al. (2015) and Yukselen and Kaya (2003). CTAB caused a significant change in mineral zeta potentials, with average values of −2.43 (kaolinite) and −8.52 mV (montmorillonite). The net negative charge of the clay particles were therefore reduced by the addition of CTAB. The SA treatments showed a similar trend for the montmorillonite (i.e., the zeta potentials of treated montmorillonite were significantly different than the untreated mineral) and for the kaolinite samples mixed with low concentrations of SA (0.5% and 5%). However, the net negative charge of the clay particles significantly increased (i.e., significant decrease in zeta potential) when kaolinite had higher SA concentrations (> 5%). This result may relate to the amount of free-phase SA in the samples.

3.4. Water Repellency

3.4.1. Solid-Water Contact Angles

The solid-water contact angle increased with the percentage of SA applied to the minerals, thus indicating increasing soil water repellency (Figure 3). The montmorillonite samples only showed hydrophobicity (i.e., contact angle ≥ 90°) for SA concentrations of 35%, while the kaolinite samples became hydrophobic for SA concentrations ≥ 5%.The CTAB-treated minerals were hydrophobic, even though relatively little CTAB was adsorbed onto the mineral surfaces compared to the SA treatments (Table 1). The kaolinite had larger solid-water contact angles than the montmorillonite for any given level of SA, which may be attributed to montmorillonite having greater surface charge and surface area (thus mitigating some of the induced repellency). Still, the montmorillonite had a larger solid-water contact angle than the kaolinite for the CTAB treatment, possibly reflecting the greater concentration of absorbed material (Table 1).

3.4.2. Water Vapor Sorption Characteristics

For both minerals, water vapor sorption isotherms showed nonlinear relationships between water content and water activity, though the isotherms differed in shape and magnitude due to different mineral structure and surface properties (Figure 4). Montmorillonite had higher water contents than kaolinite for all treatments and water activities. The addition of either hydrophobicity-inducing agent (CTAB or SA) reduced the amount of water vapor sorbed onto the minerals for a given water activity, with increasing SA concentrations associated with less water vapor sorption (Figure 4). The adsorption and desorption isotherms were both affected, meaning that the addition of hydrophobicity-inducing chemicals increased the amount of energy required to adsorb and desorb water. The montmorillonite samples showed hysteresis between adsorption and desorption curves, whereas in the kaolinite samples the adsorption and desorption curves were indistinguishable. The addition of CTAB and SA significantly decreased the hysteretic area of the montmorillonite samples, with increasing SA concentrations associated with smaller hysteretic area (Figure 5).

The isotherms were divided into three stages that represented distinct modes of water vapor sorption: (1) external monolayer adsorption ($a_w < 0.2$), (2) multilayer/interlayer adsorption ($0.2 < a_w < 0.6$), and (3) capillary condensation ($a_w \geq 0.6$). The differences in water contents over each of those activity ranges were then calculated (Figure 6). For the kaolinite treatments, significant differences in adsorption were seen for the multilayer/interlayer adsorption and capillary condensation regions, but not in the monolayer region (Figure 6a). During desorption, significant differences only occurred in the capillary condensation region (Figure 6b). Montmorillonite samples, in contrast, showed significant differences in both absorbed (Figure 6c) and desorbed (Figure 6d) water for all three regions of water activity. The control samples had significantly higher water contents than all of the treated samples, except for the monolayer regime in the 0.5% SA montmorillonite treatment.

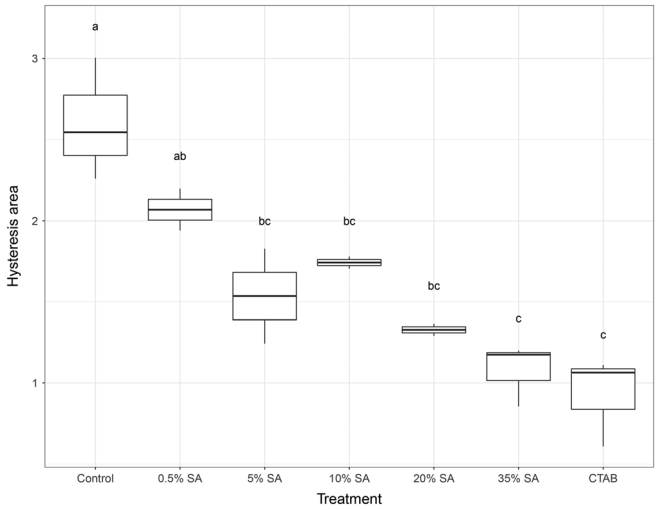

Figure 5. Hysteresis area for water activity ranges from 0.05 to 0.95 for Ca^{2+}-montmorillonite samples. Experimental treatments were 0% (control), 0.5%, 5%, 10%, 20%, and 35% of stearic acid (SA) and saturated by cetyl trimethylammonium bromide (CTAB; $n = 3$). The upper whiskers refer to the values ranging from the upper quartile to the highest data point that is less than the upper quartile plus 1.5 times the interquartile (Q3 + 1.5 IQR); the lower whiskers refer to the values ranging from the lower quartile down to the lowest data point that is greater than the lower quartile minus 1.5 times the interquartile (Q1 − 1.5 IQR). Different letters denote significant differences between mean values (ANOVA with Tukey's HSD, $p < 0.05$). ANOVA = analysis of variance; HSD = honestly significant difference.

4. Discussion

In this study, we observed that the addition of the hydrophobicity-inducing agents CTAB and SA caused montmorillonite and kaolinite minerals to become repellent to both liquid water (Figure 3) and water vapor (Figures 4 and 6). While the effects of soil water repellency on liquid water imbibition have been well studied (Leelamanie & Karube, 2007; Miller et al., 2017; Schwen et al., 2015), the latter finding provides evidence that further refutes the assumption that repellency does not affect soil vapor dynamics (Doerr et al., 2000). Our results also suggest that water vapor may be more sensitive than liquid water to low levels of hydrophobic compounds. For example, SA concentrations ≤10% did not significantly increase the solid-water contact angle in montmorillonite, whereas the amount of sorbed water vapor decreased even when SA represented only 0.5% of the sample by mass. Thus, while degree of repellency may cause a threshold-type response for liquid water imbibition (Bauters et al., 1998; Steenhuis et al., 2005), vapor sorption appears to continually decrease with increasing amount of hydrophobic agents in the clay minerals. One potential reason for this discrepancy is that water drop testing, being a small-scale imbibition process, may only show effects when a sufficient number of pores become water repellent (Bauters et al., 2000; Steenhuis et al., 2005), whereas vapor sorption depends on microscale variations in repellency.

We identified three main mechanisms by which the applied chemical treatments decreased soil vapor sorption. The chemical surface coatings (1) decreased the number and accessibility of wettable sites, as seen in low SA concentration samples (Figure S2); (2) increased aggregation (Figure 1), which likely reduced specific surface area; and (3) reduced particle surface free energy (zeta potential) of the mineral surfaces, which led to reduced van der Waals and acid-base interactions with water (Figure 2). These three changes inhibited the ability of the mineral surfaces to adsorb water vapor (Figure 4). The relative importance of these mechanisms appears to vary between minerals and hydrophobicity-inducing agents, depending on the interaction modes between each mineral and counter agent (Figure 7). While both molecules used to induce soil water repellency were amphiphilic (i.e., one hydrophobic and one hydrophilic end), the charges of the polar ends were different for each. The CTAB molecules have a positive (cation) end that can replace calcium ions. In addition, the CTAB molecules may have penetrated into the interlayer space of montmorillonite (a 2:1 mineral), forming interlayer hydrophobic complexes with quasi-crystalline structure (Shang et al., 2002). The SA molecule has a negative (anion) end, but in its acid form likely only coated the external mineral surface through electrostatic attraction facilitated by bridging calcium cations. The strength and stability of the mineral surface-calcium-SA linkages were much weaker than the strength of mineral surface CTAB bonds. Moreover, diethyl ether, the organic solvent used in the SA treatments, likely promoted the montmorillonite 2:1 layers to collapse together (Song & Sandí, 2001). After the subsequent removal of diethyl ether via evaporation, water vapor molecules could again diffuse into the interlayer space. As a result, even though the CTAB-saturated montmorillonite had nearly identical carbon content as the 5% SA montmorillonite treatment (Table 1), the water vapor sorption curves of these minerals had different shapes, with the CTAB-treated samples having significantly lower water contents (Figure 4) and hysteretic areas (Figure 5). These differences were also reflected by the solid-water contact angles: 130° for the CTAB-treated montmorillonite versus 0° for the 5% SA montmorillonite treatment. Thus, even though both treatments had approximately the same mass of adsorbed chemical (~3.5%), the CTAB samples showed hydrophobicity (i.e., contact angle ≥ 90°) while the SA samples showed hydrophilicity (i.e., contact angle ≈ 0°).

By contrast, kaolinite—a 1:1 mineral that lacks interlayer space—did not show significant differences in adsorbed and desorbed water vapor between the CTAB and 5% SA treatments (Figures 4 and 6). The solid-water contact angle for the CTAB-treated kaolinite (90°) fell between the contact angles for the 0.5% and

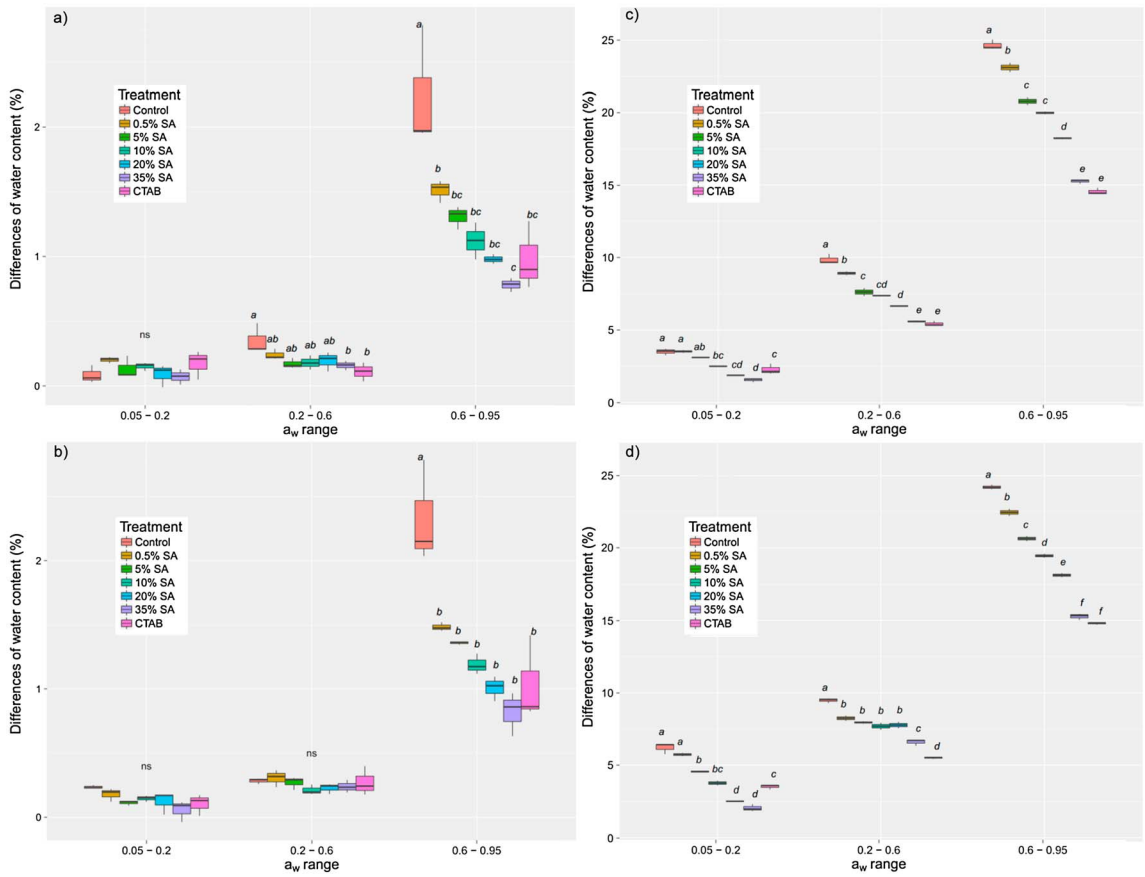

Figure 6. Differences between maximum and minimum water content for three water activity ranges (0.05–0.2, 0.2–0.6, 0.6–0.95), for Ca^{2+}-kaolinite samples undergoing (a) adsorption and (b) and desorption, and for Ca^{2+}-montmorillonite samples undergoing (c) adsorption and (d) desorption. Experimental treatments were 0% (control), 0.5%, 5%, 10%, 20%, and 35% of stearic acid (SA) and saturated by cetyl trimethylammonium bromide (CTAB) ($n = 3$). The upper whiskers refer to the values ranging from the upper quartile to the highest data point that is less than the upper quartile plus 1.5 times the interquartile (Q3 + 1.5 IQR); the lower whiskers refer to the values ranging from the lower quartile down to the lowest data point that is greater than the lower quartile minus 1.5 times the interquartile (Q1 − 1.5 IQR). Different letters denote significant differences between mean values, while *ns* denotes no significant differences between treatments (ANOVA with Tukey's HSD, $p < 0.05$). ANOVA = analysis of variance; HSD = honestly significant difference.

5% SA treatments (Figure 3), meaning that the contact angle roughly scaled with the mass of adsorbed chemical (Table 1). Because kaolinite has relatively few sorption sites due to its low-specific surface area and surface charge, the SA molecules condensed at high concentrations into a free phase (Figure S2) and joined small clay particles together into larger aggregates (Figure 1; Piccolo & Mbagwu, 1999). Both of these factors reduced the specific surface area of the mineral, as well as its ability to sorb vapor.

The distinct modes of chemical-mineral interaction also influenced vapor sorption dynamics. In our analysis, we conceptually divided the vapor sorption isotherms into three domains: external monolayer coverage ($a_w \leq 0.2$), multilayer/interlayer coverage ($0.2 < a_w < 0.6$), and capillary condensation ($a_w \geq 0.6$). The montmorillonite showed significant reductions in sorbed water for all three domains, while the kaolinite only showed differences for multilayer adsorption and the capillary condensation region. The effect of the induced repellency on the monolayer water coverage on kaolinite was not significant, as the low surface area and negligible charge of that mineral may have caused any effects to be below the instrument detection limits. Both minerals showed the greatest reduction in adsorbed and desorbed water vapor in the capillary condensation range, suggesting that soil water repellency can weaken the adhesion force that drives capillary water condensation (Philip, 1977). For kaolinite, the significant reduction of adsorbed water contents in kaolinite samples for $a_w > 0.6$ may imply that addition of hydrophobicity-inducing agents prevented cation dissociation and hydration (Hatch et al., 2012). For montmorillonite, the decrease in hysteretic areas for the treated minerals (Figure 5) may be due to a reduction in cation hydration, where the nonunique

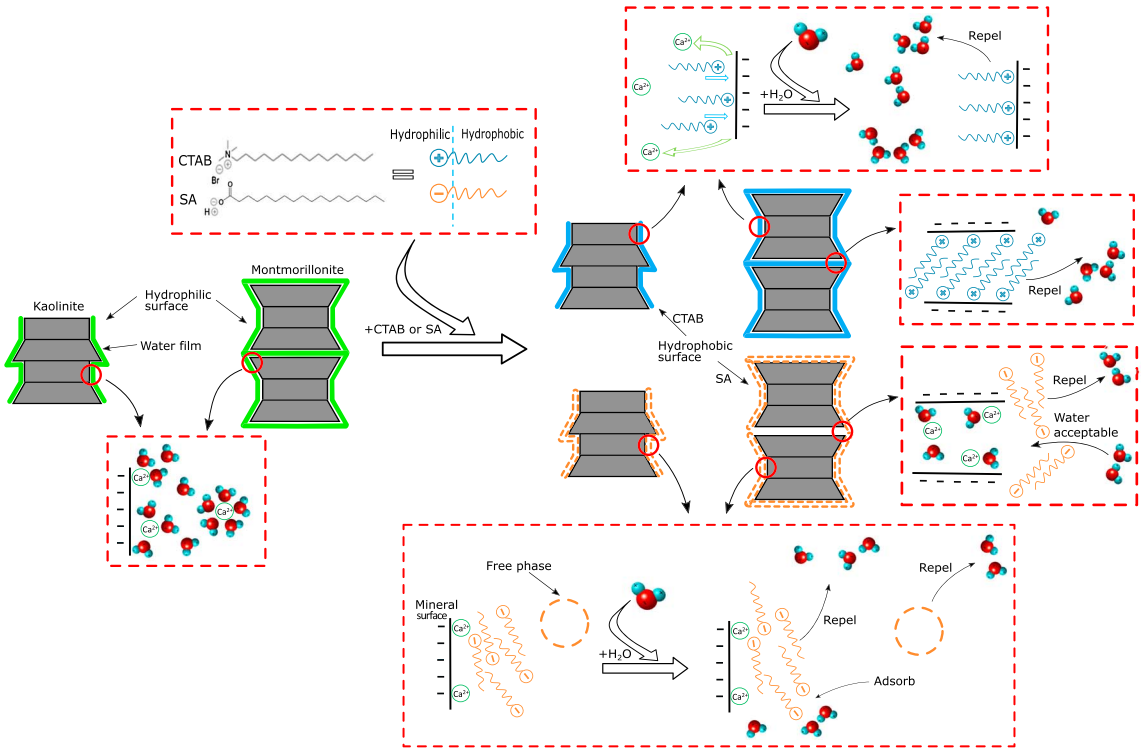

Figure 7. Conceptual model of interactions between hydrophobicity-inducing agents (CTAB and SA) and kaolinite and montmorillonite surfaces, and subsequent effect on water vapor sorption. SA = stearic acid; CTAB = cetyl trimethylammonium bromide.

energy associated with the hydration and dehydration of exchangeable cations is a primary cause of water vapor sorption hysteresis (Lu & Khorshidi, 2015).

Integrated together, these findings imply that water repellent surfaces can prevent vapor sorption and condensation, meaning that more water will remain in the vapor phase as soil water repellency increases. In natural soils, repellency often breaks down at high water contents (de Jonge et al., 2007), so the reduced ability to condense water vapor may represent a positive feedback by which hydrophobic conditions are maintained even in relatively humid conditions. This mechanism may also pertain to previous observations showing that air humidity and liquid solid-water contact angles were positively correlated (i.e., greater contact angles were observed at higher air humidity; Whelan et al., 2015). Still, the Whelan et al. (2015) study observed this relationship for sand particles that had been treated with SA yet not in natural dune sand particles, meaning that these results could be artifacts arising from the use of pure minerals and hydrophobicity-inducing chemicals. Similar caution may be warranted when extending the findings of the present study, which used model minerals, to natural soils. Still, kaolinite and montmorillonite minerals represent two of the most common clay minerals found worldwide (Ito & Wagai, 2017), while SA is a common organic component within the soil environment (Deng & Dixon, 2002). The amphiphilic nature of both SA and CTAB also means that these chemicals represent the dominant molecular structure found in soil organic matter (Kleber & Johnson, 2010). While these factors all imply the study should have relevance to natural systems, future investigations still should examine whether these mechanisms occur within real soils.

5. Summary and Conclusion

To elucidate the mechanisms and magnitudes of how soil water repellency affects vapor sorption, we treated kaolinite and montmorillonite minerals with one of two hydrophobicity-inducing agents (SA and CTAB) and then measured their water vapor sorption dynamics. The water repellent treatments reduced water vapor sorption in proportion to the mass of applied chemicals. The montmorillonite samples showed differences in sorption throughout the entire range of water contents, whereas the kaolinite samples only differed in

the high range of water activities ($a_w > 0.6$), where water vapor typically condenses due to capillary attraction. Water repellent surfaces therefore may act to prevent water vapor sorption and condensation. Compared to liquid water, vapor had greater sensitivity to low concentrations of hydrophobicity-inducing agents, as the montmorillonite samples showed significantly reduced water vapor sorption yet no differences in solid-water contact angles for SA concentrations ≤5% by mass. By extension, hydrophobicity-inducing chemicals in minerals can affect water retention even if they are not concentrated enough to inhibit infiltration.

Upscaling these findings, by lowering the surface potential of soil particles and reducing available sorption sites, soil water repellency may accelerate water vapor losses from mineral soils. These effects may be most notable when water evaporation reaches the vapor diffusion stage (i.e., stage III evaporation), where the reduced ability to condense and store water may increase vapor pressure gradients that drive transport. While more study is needed to examine whether these mechanisms translate to natural soils, soil water repellency may be a concern in arid or drought-stricken regions not only for its influence on soil infiltration capacity but also for its potential to encourage water vapor losses.

Acknowledgments
Data from this paper are permanently archived at https://data.lib.vt.edu/files/9g54xh74w. Support for this project came from the Virginia Tech Institute for Critical Technology and Applied Science (VT-ICTAS). Funding for this work was provided in part by the Virginia Agricultural Experiment Station and the Hatch Program of the National Institute of Food and Agriculture, U.S. Department of Agriculture.

References

Abatzoglou, J. T., & Williams, A. P. (2016). Impact of anthropogenic climate change on wildfire across western US forests. *Proceedings of the National Academy of Sciences of the United States of America*, *113*(42), 11,770–11,775. https://doi.org/10.1073/pnas.1607171113

Arthur, E., Tuller, M., Moldrup, P., & de Jonge, L. W. (2014). Evaluation of a fully automated analyzer for rapid measurement of water vapor sorption isotherms for applications in soil science. *Soil Science Society of America Journal*, *78*(3), 754–760. https://doi.org/10.2136/sssaj2013.11.0481n

Arthur, E., Tuller, M., Moldrup, P., & de Jonge, L. W. (2016). Evaluation of theoretical and empirical water vapor sorption isotherm models for soils. *Water Resources Research*, *52*, 190–205. https://doi.org/10.1002/2015wr017681

Arthur, E., Tuller, M., Moldrup, P., Greve, M. H., Knadel, M., & de Jonge, L. W. (2018). Applicability of the Guggenheim–Anderson–Boer water vapour sorption model for estimation of soil specific surface area. *European Journal of Soil Science*, *69*(2), 245–255. https://doi.org/10.1111/ejss.12524

Arthur, E., Tuller, M., Moldrup, P., Jensen, D. K., & de Jonge, L. W. (2015). Prediction of clay content from water vapour sorption isotherms considering hysteresis and soil organic matter content. *European Journal of Soil Science*, *66*(1), 206–217. https://doi.org/10.1111/ejss.12191

Bachmann, J., Ellies, A., & Hartge, K. (2000). Development and application of a new sessile drop contact angle method to assess soil water repellency. *Journal of Hydrology*, *231-232*, 66–75. https://doi.org/10.1016/S0022-1694(00)00184-0

Bauters, T. W., Steenhuis, T. S., DiCarlo, D., Nieber, J., Dekker, L., Ritsema, C., et al. (2000). Physics of water repellent soils. *Journal of Hydrology*, *231-232*, 233–243. https://doi.org/10.1016/S0022-1694(00)00197-9

Bauters, T. W., Steenhuis, T. S., Parlange, J.-Y., & DiCarlo, D. A. (1998). Preferential flow in water-repellent sands. *Soil Science Society of America Journal*, *62*(5), 1185–1190. https://doi.org/10.2136/sssaj1998.03615995006200050005x

Branson, K., & Newman, A. (1983). Water sorption on Ca-saturated clays: I. Multilayer sorption and microporosity in some illites. *Clay Minerals*, *18*(3), 277–287. https://doi.org/10.1180/claymin.1983.018.3.05

Dagnelie, R. V., Crassous, A., & Tran-Thi, T.-H. (2010). Scaling the hydrophobicity of porous materials to water vapour with Fluoral-P. *Journal of Membrane Science*, *365*(1-2), 98–105. https://doi.org/10.1016/j.memsci.2010.08.049

Dai, A. (2011). Drought under global warming: A review. *Wiley Interdisciplinary Reviews: Climate Change*, *2*(1), 45–65. https://doi.org/10.1002/wcc.81

Deng, Y., & Dixon, J. B. (2002). Soil organic matter and organic-mineral interactions. *Soil Mineralogy with Environmental Applications*, 69–107. https://doi.org/10.2136/sssabookser7.c3

Dennison, P. E., Brewer, S. C., Arnold, J. D., & Moritz, M. A. (2014). Large wildfire trends in the western United States, 1984–2011. *Geophysical Research Letters*, *41*, 2928–2933. https://doi.org/10.1002/2014GL059576

Derjaguin, B. V., Churaev, N. V., & Muller, V. M. (1987). Surface forces: Plenum Pub Corp. https://doi.org/10.1007/978-1-4757-6639-4

Doerr, S. H., Shakesby, R., & Walsh, R. (2000). Soil water repellency: Its causes, characteristics and hydro-geomorphological significance. *Earth-Science Reviews*, *51*(1-4), 33–65. https://doi.org/10.1016/S0012-8252(00)00011-8

Doerr, S. H., & Thomas, A. D. (2000). The role of soil moisture in controlling water repellency: New evidence from forest soils in Portugal. *Journal of Hydrology*, *231-232*, 134–147. https://doi.org/10.1016/S0022-1694(00)00190-6

Ellerbrock, R., & Gerke, H. (2016). Analyzing management-induced dynamics of soluble organic matter composition in soils from long-term field experiments. *Vadose Zone Journal*, *15*(4). https://doi.org/10.2136/vzj2015.05.0074

Gee, G. W., & Bauder, J. W. (1986). Particle-size analysis. In A. Klute (Ed.), *Methods of soil analysis. Part I, Agron. Monogr*. (2nd ed., Vol. 9, pp. 383–411). Madison, WI: ASA and SSSA.

Goebel, M. O., Bachmann, J., Reichstein, M., Janssens, I. A., & Guggenberger, G. (2011). Soil water repellency and its implications for organic matter decomposition—Is there a link to extreme climatic events? *Global Change Biology*, *17*(8), 2640–2656. https://doi.org/10.1111/j.1365-2486.2011.02414.x

Granged, A. J., Jordán, A., Zavala, L. M., & Bárcenas, G. (2011). Fire-induced changes in soil water repellency increased fingered flow and runoff rates following the 2004 Huelva wildfire. *Hydrological Processes*, *25*(10), 1614–1629. https://doi.org/10.1002/hyp.7923

Hatch, C. D., Wiese, J. S., Crane, C. C., Harris, K. J., Kloss, H. G., & Baltrusaitis, J. (2012). Water adsorption on clay minerals as a function of relative humidity: Application of BET and Freundlich adsorption models. *Langmuir*, *28*(3), 1790–1803. https://doi.org/10.1021/la2042873

Imeson, A., Verstraten, J., Van Mulligen, E., & Sevink, J. (1992). The effects of fire and water repellency on infiltration and runoff under Mediterranean type forest. *Catena*, *19*(3-4), 345–361. https://doi.org/10.1016/0341-8162(92)90008-Y

Inagaki, S., Fukushima, Y., Kuroda, K., & Kuroda, K. (1996). Adsorption isotherm of water vapor and its large hysteresis on highly ordered mesoporous silica. *Journal of Colloid and Interface Science*, *180*(2), 623–624. https://doi.org/10.1006/jcis.1996.0345

Ito, A., & Wagai, R. (2017). Global distribution of clay-size minerals on land surface for biogeochemical and climatological studies. *Scientific Data*, *4*, 170103. https://doi.org/10.1038/sdata.2017.103

de Jonge, L. W., Moldrup, P., & Jacobsen, O. H. (2007). Soil-water content dependency of water repellency in soils. *Soil Science*, *172*(8), 577–588 . https://doi.org/10.1097/SS.0b013e318065c090

Kidron, G. J. (2015). The role of crust thickness in runoff generation from microbiotic crusts. *Hydrological Processes*, *29*(7), 1783–1792. https://doi.org/10.1002/hyp.10243

Kleber, M., & Johnson, M. G. (2010). Advances in understanding the molecular structure of soil organic matter: Implications for interactions in the environment. In *Advances in Agronomy* (Vol. 106, pp. 77–142). Cambridge, MA: Academic Press. https://doi.org/10.1016/S0065-2113(10)06003-7

Laird, D. A., Shang, C., & Thompson, M. L. (1995). Hysteresis in crystalline swelling of smectites. *Journal of Colloid and Interface Science*, *171*(1), 240–245. https://doi.org/10.1006/jcis.1995.1173

Larsen, I. J., MacDonald, L. H., Brown, E., Rough, D., Welsh, M. J., Pietraszek, J. H., et al. (2009). Causes of post-fire runoff and erosion: Water repellency, cover, or soil sealing? *Soil Science Society of America Journal*, *73*(4), 1393–1407. https://doi.org/10.2136/sssaj2007.0432

Leão, T. P., & Tuller, M. (2014). Relating soil specific surface area, water film thickness, and water vapor adsorption. *Water Resources Research*, *50*, 7873–7885. https://doi.org/10.1002/2013WR014941

Leelamanie, D., & Karube, J. (2007). Effects of organic compounds, water content and clay on the water repellency of a model sandy soil. *Soil Science & Plant Nutrition*, *53*(6), 711–719. https://doi.org/10.1111/j.1747-0765.2007.00199.x

Leelamanie, D., Karube, J., & Yoshida, A. (2008). Characterizing water repellency indices: Contact angle and water drop penetration time of hydrophobized sand. *Soil Science & Plant Nutrition*, *54*(2), 179–187. https://doi.org/10.1111/j.1747-0765.2007.00232.x

Leroy, P., Tournassat, C., Bernard, O., Devau, N., & Azaroual, M. (2015). The electrophoretic mobility of montmorillonite. Zeta potential and surface conductivity effects. *Journal of Colloid and Interface Science*, *451*, 21–39. https://doi.org/10.1016/j.jcis.2015.03.047

Letey, J. (2001). Causes and consequences of fire-induced soil water repellency. *Hydrological Processes*, *15*(15), 2867–2875. https://doi.org/10.1002/hyp.378

Lichner, L., Dlapa, P., Doerr, S. H., & Mataix-Solera, J. (2006). Evaluation of different clay minerals as additives for soil water repellency alleviation. *Applied Clay Science*, *31*(3–4), 238–248. https://doi.org/10.1016/j.clay.2005.10.012

Lin, C., Fan, B., Zhang, J. X., Yang, X., & Zhang, H. (2016). Study on lead ion wastewater treatment of self-assembled film. *Desalination and Water Treatment*, *57*(45), 21,627–21,633. https://doi.org/10.1080/19443994.2015.1121839

Lu, N., & Khorshidi, M. (2015). Mechanisms for soil-water retention and hysteresis at high suction range. *Journal of Geotechnical and Geoenvironmental Engineering*, *141*(8), 04015032. https://doi.org/10.1061/(ASCE)GT.1943-5606.0001325

Maaz, S., Rose, M., & Palkovits, R. (2016). Systematic investigation of the pore structure and surface properties of SBA-15 by water vapor physisorption. *Microporous and Mesoporous Materials*, *220*, 183–187. https://doi.org/10.1016/j.micromeso.2015.09.005

Miller, J. J., Beasley, B. W., Hazendonk, P., Drury, C. F., & Chanasyk, D. S. (2017). Influence of long-term application of feedlot manure amendments on water repellency of a clay loam soil. *Journal of Environmental Quality*, *46*(3), 667–675. https://doi.org/10.2134/jeq2017.02.0074

Miyamoto, S., Letey, J., & Osborn, J. (1972). Water vapor adsorption by water-repellent soils at equilibrium. *Soil Science*, *114*(3), 180–184. https://doi.org/10.1097/00010694-197209000-00004

Miyata, S., Kosugi, K. i., Gomi, T., Onda, Y., & Mizuyama, T. (2007). Surface runoff as affected by soil water repellency in a Japanese cypress forest. *Hydrological Processes*, *21*(17), 2365–2376. https://doi.org/10.1002/hyp.6749

Newman, A. (1983). The specific surface of soils determined by water sorption. *Journal of Soil Science*, *34*(1), 23–32. https://doi.org/10.1111/j.1365-2389.1983.tb00809.x

Nobrega, M. M., Olivato, J. B., Müller, C. M., & Yamashita, F. (2012). Biodegradable starch-based films containing saturated fatty acids: Thermal, infrared and Raman spectroscopic characterization. *Polímeros*, *22*(5), 475–480. https://doi.org/10.1590/S0104-14282012005000068

Orfanus, T., Dlapa, P., Fodor, N., Rajkai, K., Sandor, R., & Novakova, K. (2014). How severe and subcritical water repellency determines the seasonal infiltration in natural and cultivated sandy soils. *Soil and Tillage Research*, *135*, 49–59. https://doi.org/10.1016/j.still.2013.09.005

Ormerod, E., & Newman, A. (1983). Water sorption on Ca-saturated clays: II. Internal and external surfaces of montmorillonite. *Clay Minerals*, *18*(03), 289–299. https://doi.org/10.1180/claymin.1983.018.3.06

Parks, G. A. (1984). Surface and interfacial free energies of quartz. *Journal of Geophysical Research*, *89*(B6), 3997–4008. https://doi.org/10.1029/JB089iB06p03997

Philip, J. (1977). Unitary approach to capillary condensation and adsorption. *The Journal of Chemical Physics*, *66*(11), 5069–5075. https://doi.org/10.1063/1.433814

Piccolo, A., & Mbagwu, J. S. (1999). Role of hydrophobic components of soil organic matter in soil aggregate stability. *Soil Science Society of America Journal*, *63*(6), 1801–1810. https://doi.org/10.2136/sssaj1999.6361801x

Prunty, L., & Bell, J. (2007). Soil water hysteresis at low potential. *Pedosphere*, *17*(4), 436–444. https://doi.org/10.1016/S1002-0160(07)60053-8

Puri, B. R., & Murari, K. (1964). Studies in surface area measurements of soils: 2. Surface area from a single point on the water isotherm. *Soil Science*, *97*(5), 341–343. https://doi.org/10.1097/00010694-196405000-00008

Quirk, J. (1955). Significance of surface areas calculated from water vapor sorption isotherms by use of the BET equation. *Soil Science*, *80*(6), 423–430. https://doi.org/10.1097/00010694-195512000-00001

Quirk, J., & Murray, R. (1999). Appraisal of the ethylene glycol monoethyl ether method for measuring hydratable surface area of clays and soils. *Soil Science Society of America Journal*, *63*(4), 839–849. https://doi.org/10.2136/sssaj1999.634839x

Ritsema, C. J., Dekker, L. W., Hendrickx, J. M. H., & Hamminga, W. (1993). Preferential flow mechanism in a water repellent sandy soil. *Water Resources Research*, *29*(7), 2183–2193. https://doi.org/10.1029/93wr00394

Santos, D., Costa, F., Franceschi, E., Santos, A., Dariva, C., & Mattedi, S. (2014). Synthesis and physico-chemical properties of two protic ionic liquids based on stearate anion. *Fluid Phase Equilibria*, *376*, 132–140. https://doi.org/10.1016/j.fluid.2014.05.043

Schneider, M., & Goss, K.-U. (2012). Prediction of the water sorption isotherm in air dry soils. *Geoderma*, *170*, 64–69. https://doi.org/10.1016/j.geoderma.2011.10.008

Schwen, A., Zimmermann, M., Leitner, S., & Woche, S. K. (2015). Soil water repellency and its impact on hydraulic characteristics in a beech forest under simulated climate change. *Vadose Zone Journal*, *14*(12). https://doi.org/10.2136/vzj2015.06.0089

Shang, C., Rice, J., & Lin, J. (2002). Small-angle X-ray scattering study of the quasi-crystal structure of montmorillonite-CTAB in suspension. *Soil Science Society of America Journal*, *66*(4), 1225–1230. https://doi.org/10.2136/sssaj2002.1225

Simkovic, I., Dlapa, P., Doerr, S. H., Mataix-Solera, J., & Sasinkova, V. (2008). Thermal destruction of soil water repellency and associated changes to soil organic matter as observed by FTIR spectroscopy. *Catena*, *74*(3), 205–211. https://doi.org/10.1016/j.catena.2008.03.003

Song, K., & Sandí, G. (2001). Characterization of montmorillonite surfaces after modification by organosilane. *Clays and Clay Minerals*, *49*(2), 119–125. https://doi.org/10.1346/CCMN.2001.0490202

Steenhuis, T. S., Hunt, A. G., Parlange, J. Y., & Ewing, R. P. (2005). Assessment of the application of percolation theory to a water repellent soil. *Australian Journal of Soil Research*, *43*(3), 357. https://doi.org/10.1071/sr04093

Tuller, M., & Or, D. (2005). Water films and scaling of soil characteristic curves at low water contents. *Water Resources Research*, *41*, W09403. https://doi.org/10.1029/2005WR004142

Valolahti, H., Kivimäenpää, M., Faubert, P., Michelsen, A., & Rinnan, R. (2015). Climate change-induced vegetation change as a driver of increased subarctic biogenic volatile organic compound emissions. *Global Change Biology*, *21*(9), 3478–3488. https://doi.org/10.1111/gcb.12953

Whelan, A., Kechavarzi, C., Coulon, F., & Doerr, S. H. (2015). Experimental characterization of the impact of temperature and humidity on the breakdown of soil water repellency in sandy soils and composts. *Hydrological Processes*, *29*(8), 2065–2073. https://doi.org/10.1002/hyp.10305

Woodruff, W., & Revil, A. (2011). CEC-normalized clay-water sorption isotherm. *Water Resources Research*, *47*, W11502. https://doi.org/10.1029/2011WR010919

Yeşilbaş, M., & Boily, J.-F. (2016). Particle size controls on water adsorption and condensation regimes at mineral surfaces. *Scientific Reports*, *6*(1), 32136. https://doi.org/10.1038/srep32136

Youssef, H., Ali, Z., El-Nemr, K., & Bekhit, M. (2013). Effect of ionizing radiation on the properties of acrylonitrile butadiene rubber/clay nanocomposites. *Journal of Elastomers & Plastics*, *45*(5), 407–428. https://doi.org/10.1177/0095244312457797

Yukselen, Y., & Kaya, A. (2003). Zeta potential of kaolinite in the presence of alkali, alkaline Earth and hydrolyzable metal ions. *Water, Air, and Soil Pollution*, *145*(1), 155–168. https://doi.org/10.1023/A:1023684213383

Zhu, L., Ren, X., & Yu, S. (1998). Use of cetyltrimethylammonium bromide-bentonite to remove organic contaminants of varying polar character from water. *Environmental Science & Technology*, *32*(21), 3374–3378. https://doi.org/10.1021/es980353m